A Robust Approach for Estimating Diffusion Constants from Concentration Data in Microchannel Mixers

Carlos Pinto Coelho cfspc@mit.edu
Salil Desai desai@mit.edu
Dennis Freeman freeman@mit.edu
Jacob White white@mit.edu
Massachusetts Institute of Technology - Research Laboratory of Electronics

ABSTRACT

In this paper we present a robust and geometry independent method for the estimation of diffusion coefficients of solutes from image data. Our diffusion coefficient estimation algorithm works in two steps. First, given the device geometry and the pressure boundary conditions, we calculate the fluid velocity in the device by solving a Stokes flow problem. Then, using the calculated fluid velocity and the concentration at the device inlet and outlet ports we calculate the solute concentration in the device by solving the convection diffusion problem with a finite differences solver. The diffusion coefficient is estimated by using Newton's method to minimize the square error between the measured concentration data and the concentration estimates produced with our simulation tool.

keywords: convection-diffusion, parameter extraction.

1 INTRODUCTION

In this paper we present an algorithm for estimating the diffusion coefficient of a solute using microfluidic mixers and image data. Our estimation technique starts by simulating the convection process for the specific mixer topology. The fluid convection is assumed to be independent of the solute concentration and is calculated by solving a Stokes flow problem. Given the fluid velocity profile inside the mixer and the solute concentration at the mixer inlet ports, we use a finite-differences solver to calculate the solute concentration along the mixer. An estimate of the diffusion coefficient is generated by minimizing the difference between the concentration values calculated through simulation and the concentration values obtained from the image data. To perform the minimization we used Newton's method and developed an efficient way of calculating the sensitivity of the simulated concentration values to changes in the diffusion coefficient. We compared the diffusion coefficient estimates generated with our algorithm with diffusion coefficient estimates calculated using two other approaches and show that our algorithm is more robust in dealing with noisy data and with narrow channels, where Taylor dispersion is more important.

Using our simulation tools to estimate diffusion coefficients is an indirect way of validating them and illustrating their effectiveness in predicting concentration profiles in devices that may have complicated geometries. The study of diffusion in non-uniform flows is important for several applications. For example, in [1] and [2] topology modifications are proposed to reduce convection enhanced diffusion, also known as Taylor dispersion, for lab-on-a-chip applications. As another example, in [3] topologies are explored to promote diffusion and mixing.

2 METHODS

2.1 Experimental setup

Our test setup used gravity driven Y-shaped PDMS microfluidic mixers as illustrated in Figure 1 and further described in [4]. The mixers consist of two input channels that are 25mm long and that are connected to an output channel that is 35mm long. We used two mixers, one with a channel width of 250μm and another with a channel width of 500μm; in both cases the channel depth was 75μm. A solution containing Allura Red was placed in one of the mixer inlets and clear water was placed on the other inlet; the outlet port was empty. After a steady state was reached, we collected several images along the mixer outlet channel using a CCD camera (Unibrain Fire-i400 Firewire Industrial). The images were captured using a 4$\times$ objective and the scene was lit by trans-illumination using a LED (Luxeon Star white emitter).

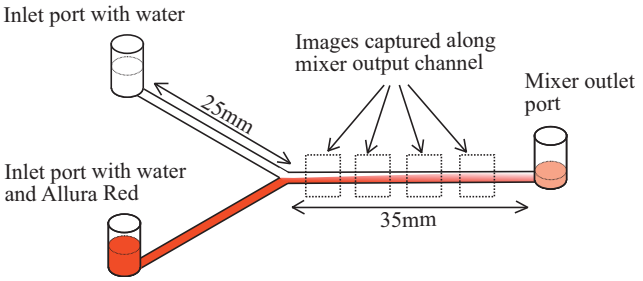

Figure 1: Experimental setup: A solution containing Allura Red food dye was placed in one of the inlet while the same height of clear water was placed on the other inlet. Images were collected along the mixer output channel and then converted to concentration value profiles that were used in the fitting algorithm to estimate the diffusion coefficient.

2.2 Beer-Lambert's law, transmittance and concentration

To relate the solute concentration to the observed RGB values we use Beer-Lambert's law. Beer-Lambert's law states

that as *monochromatic* light with a wavelength of λ goes through a sample of thickness H with a small uniform concentration, c_A, of a solute A the transmitted power P is given by

$$P(\lambda) = P_0(\lambda)e^{-\epsilon_A(\lambda)c_A H} \quad (1)$$

where $\epsilon_A(\lambda)$ is the molar extinction coefficient of solute A at the the wavelength λ and P_0 is the transmitted power in the absence of the solute A.

Even though we did not use a monochromatic light source, the power emitted by the light source has a sharp maximum in the active region of the blue CCD sensor and, for concentrations of Allura Red below 10 mM, the power measured by the blue sensor depends exponentially on the concentration value. A normalized concentration value $kc_m(x,y)$ can be obtained using

$$\begin{aligned} B(x,y) &= B_{\text{ref}}e^{-kc_m}(x,y) \\ kc_m(x,y) &= \log(B(x,y)) - \log(B_{\text{ref}}), \end{aligned} \quad (2)$$

where B_{ref} is the intensity value measured in the absence of the dye.

2.3 Convection Model - Stokes flow

Due to the small length-scales and the low fluid velocities in the mixer, viscous forces dominate the fluid transport dynamics that can therefore be modeled using the Stokes flow equations

$$\mu\nabla^2\mathbf{U} = -\nabla P, \quad (3)$$

where $\mathbf{U}$ is the vector fluid velocity and P is the pressure. To solve (3) for $\mathbf{U}$ we setup pressure boundary conditions at the mixer inlet and outlet ports and non-penetration no-slip boundary conditions at the mixer channel walls. For channels with a constant cross-section, the fluid velocity becomes laminar along the output channel and $\mathbf{U}(x,y,z) = (0, U_y(x,z), 0)$ where x is the direction along the channel width, y is the direction along the output channel and z is the direction along the channel depth. The velocity profile $U_y(x,z)$ can be calculated by solving a 2D Poisson equation driven by a constant pressure drop. Since the mixer is composed of connected constant section channels, the pressure drop across each the input and output channels can be calculated using a fluidic network model. For devices with more complicated geometries fast integral solvers, such as FastStokes [5], can be used to efficiently calculate the detailed velocity profile inside the device.

2.4 Convection-Diffusion

In the presence of only convection and diffusion, the time rate of change of the solute concentration is given by the negative divergence of the diffusive solute flux, $\mathbf{F}_D$, and the convective solute flux, $\mathbf{F}_C$. The solute flux due to diffusion is given by $\mathbf{F}_D = -D\nabla c$, where D is the unknown diffusion coefficient and c is the solute concentration. The solute flux due to convective transport is $\mathbf{F}_C = \mathbf{U}c$. In steady state, for small time-scales, the amount of solute that is transported by the diffusive and convective fluxes is in balance and the time rate of change of concentration is zero and we get

$$\frac{\partial c}{\partial t} = -\nabla\cdot(-D\nabla c + \mathbf{U}c) = 0. \quad (4)$$

Assuming that D is homogeneous and independent of concentration and that the fluid is incompressible, steady state convection-diffusion can be modeled by

$$D\nabla^2 c - \mathbf{U}\cdot\nabla c = 0. \quad (5)$$

To estimate the concentration of the solute inside our device, for a specified D, we discretize (5) using finite-differences to approximate the laplacian, the gradient and the boundary condition terms. In our simulation we use the velocity profile $\mathbf{U}(x,y,z)$ calculated in section 2.3 and enforce no-flux boundary conditions on the device walls by imposing that $\mathbf{n}_{\text{wall}}\cdot\nabla c = 0$. Since our aim is to estimate D, we match the simulated and measured values at a point y_0 near the beginning of output channel $c(x,y_0,z) = c_m(x,y_0)$ and solve the discretized (5) along the output channel. Since (5) is linear in the concentration we normalize the measured and simulated concentration values such that their maximum value is 1.

We can represent the discretized approximation to (5) by the following system of linear equations

$$\underbrace{\left[D\begin{bmatrix}\mathbf{L}_{i,i} & \mathbf{L}_{i,w} & \mathbf{L}_{i,y_0}\\ \mathbf{0} & \mathbf{0} & \mathbf{0}\\ \mathbf{0} & \mathbf{0} & \mathbf{0}\end{bmatrix}\right]}_{\mathbf{L}_s} - \underbrace{\begin{bmatrix}\mathbf{U}\cdot\nabla_{i,i} & \mathbf{U}\cdot\nabla_{i,w} & \mathbf{U}\cdot\nabla_{i,y_0}\\ \mathbf{0} & \mathbf{n}_w\cdot\nabla c_w & \mathbf{0}\\ \mathbf{0} & \mathbf{0} & \mathbf{I}_{y_0}\end{bmatrix}}_{\mathbf{U}\mathbf{G}_s}\begin{bmatrix}\mathbf{c}_{s,i}\\ \mathbf{c}_{s,w}\\ \mathbf{c}_{s,y_0}\end{bmatrix} = \begin{bmatrix}\mathbf{0}\\ \mathbf{0}\\ \mathbf{c}_{m,y_0}\end{bmatrix} \quad (6)$$

where the i, w and y_0 subscripts refer to interior grid point, to a point on the wall or to a point on $y = y_0$ where the simulation is "initialized". $\mathbf{L}_{i,w}$ refers to the contribution of the values of c on the wall to the approximation of the laplacian at an interior point. For finite-differences approximations of the differential operators the $\mathbf{L}_{i,*}$ matrices and the $\mathbf{U}\cdot\nabla_{i,*}$ matrices are very sparse.

Solving (6) produces $\mathbf{c}_s(x,y,z)$ simulated concentration values for the set of simulation grid points $(\mathbf{x}_s, \mathbf{y}_s, \mathbf{z}_s)$. To compare the simulated concentration profiles with the measured concentration values $\mathbf{c}_m$ we can average $\mathbf{c}_s(x,y,z)$ along the channel depth, z, and interpolate the simulated results from the simulation grid to the, usually coarser and sometimes irregular, measurement positions $(\mathbf{x}_m, \mathbf{y}_m)$. This interpolation operation is represented in matrix form as $\mathbf{c}_s(D, \mathbf{x}_m, \mathbf{y}_m) = \mathbf{M}_{m,s}\mathbf{c}_s(D, \mathbf{x}_s, \mathbf{y}_s)$. In our experimental setup, operating velocities and diffusivities were such that the dye concentration $\mathbf{c}_s(x,y,z)$ does not vary significantly along the z direction and we can, much more cheaply, solve a two dimensional version of (6) and obtain $\mathbf{c}_s(D, \mathbf{x}_s, \mathbf{y}_s)$ directly.

2.5 Parameter extraction through data fitting

We propose estimating D by matching the simulated concentration values $\mathbf{c}_s(D, \mathbf{x}_m, \mathbf{y}_m)$ to the measured concentration values $\mathbf{c}_s(D, \mathbf{x}_m, \mathbf{y}_m)$ by minimizing

$$\|\mathbf{E}(D)\|_2^2 = \|\mathbf{M}_{m,s}\mathbf{c}_s(D, \mathbf{x}_s, \mathbf{y}_s) - \mathbf{c}_m(\mathbf{x}_m, \mathbf{y}_m)\|_2^2. \quad (7)$$

We propose using Newton's method to perform the minimization because we found that, for this problem, it converges to a fixed value of D in a small number of iterations which reduces the number of times that we need to solve (6). Newton's method starts with a guess for D and generates a new estimate $\mathrm{D_{new}}$ using

$$\|\mathbf{E}(D_{\mathrm{old}}\|_2^2 + \frac{\partial\|\mathbf{E}\|_2^2}{\partial D}(D_{\mathrm{old}})(D_{\mathrm{new}} - D_{\mathrm{old}}) = 0 \qquad (8)$$

where

$$\frac{\partial\|\mathbf{E}\|_2^2}{\partial D}(D) = 2\mathbf{E}(D)\mathbf{M}\frac{\partial\mathbf{c_s}}{\partial D}(D). \qquad (9)$$

The value of $\frac{\partial\mathbf{c_s}}{\partial D}(D)$ can be obtained by taking the derivative of (6) with respect to D and solving

$$(D\mathbf{L_s} - \mathbf{UG_s})\frac{\partial\mathbf{c_s}}{\partial D}(D) = -\mathbf{L_s}\mathbf{c_s} \qquad (10)$$

which requires factoring the *same* matrix that was already factored to calculate $\mathbf{c_s}$ in (6). Since we are dealing with sparse matrices we can reuse the matrix factorization and generate $\frac{\partial\mathbf{c_s}}{\partial D}$ at the cost of a matrix vector product, a backward and a forward substitution. In the following we refer to the estimates produced using this method as $\mathrm{D_{FD}}$ because of the use of finite-differences in (6).

2.6 Fitting a uniform velocity model

We can generate an estimate of the diffusion coefficient $\mathrm{D_{erf}}$ by using a simplified model with a closed analytical solution that does not require solving a system of equations like (6) to generate an estimate of the solute concentration in the channel. For a rectangular channel, under the simplifying assumption that the fluid velocity is laminar and uniform along the channel cross-section, the solute concentration is

$$c(D,x,y) = \frac{C}{2} - \frac{C}{2}\mathrm{erf}\left(\frac{x - x_0}{2\sqrt{(Dt)_0 + D(y-y_0)/U_y}}\right). \qquad (11)$$

The estimate $\mathrm{D_{erf}}$ we first choose C and $(Dt)_0$ such that $c(D,x,y_0)$ matches the measured concentration values at y_0; we then use Newton's method to choosing $\mathrm{D_{erf}}$ that minimizes the square error between $c(\mathrm{D_{erf}},x,y)$ and the measured concentration values for the remaining concentration measurements. The average velocity U_y can be calculated by averaging the result produced in section 2.3.

2.7 Parameter extraction through PDE residue minimization

Alternatively, instead of iteratively solving (6) and choosing $\mathrm{D_{FD}}$ by minimizing (8), we can *choose* D_{LLS} *such that the measured concentration values satisfy the differential equation* (5) *as closely as possible*. Since we only have a discrete set of measured concentration values we cannot apply the differential operators directly to the data, instead we approximate the operators by using finite-difference schemes and get

$$\tilde{\mathbf{E}}(D) = (D\mathbf{L_m} - \mathbf{UG_m})\mathbf{c_m}, \qquad (12)$$

where $\mathbf{L_m}$ is the discrete approximation to the laplacian and $\mathbf{UG_m}$ is the discrete approximation to the dot product between the velocity component at each point and the discrete approximation to the gradient at that point. The estimate $D_{\mathrm{LLS}} = \mathrm{argmin}(\|\tilde{\mathbf{E}}(D)\|_2^2)$, where LLS stands for linear least squares, is

$$D_{\mathrm{LLS}} = ((\mathbf{L_m}\mathbf{c_m})^T(\mathbf{UG_m}\mathbf{c_m}))/\|\mathbf{L_m}\mathbf{c_m}\|_2^2. \qquad (13)$$

3 RESULTS AND DISCUSSION

Before comparing the diffusion coefficient estimates produced by the methods proposed in the previous sections we introduce a reference value for the Allura Red diffusion coefficient $\mathrm{D_{AR}} = 4.34\times10^{-6}\mathrm{cm^2s^{-1}}$. This reference value $\mathrm{D_{AR}}$ was calculated using Einstein's relation [6] that relates the molar mass of a solute with its diffusion coefficient.

The diffusion coefficient estimates produced using each of the methods presented in sections 2.5, 2.6 and 2.7 are summarized in Table 1. Our first observation is that the method of choosing D_{LLS} to minimize the residue of the differential equation applied to the measured data, presented in section 2.7, does not produce consistent or even physically valid estimates of D. In contrast, the methods presented in sections 2.5 and 2.6, based on matching simulated concentration values to measured concentration values, produce $\mathrm{D_{FD}}$ and $\mathrm{D_{erf}}$ that are of the same order of magnitude as D_{AR}. Furthermore, the estimates $\mathrm{D_{FD}}$ generated using data collected for both 500μm and 250μm wide channels are consistent with each other and are within 30% of $\mathrm{D_{AR}}$.

Table 1: Estimates for the Allura Red diffusion coefficient (reference value $\mathrm{D_{AR}} = 4.34\times10^{-6}\mathrm{cm^2s^{-1}}$). For $\mathrm{D_{FD}}$ see section 2.5, for $\mathrm{D_{erf}}$ see section 2.6 and for $\mathrm{D_{LLS}}$ see section 2.7.

data set	W [μm]	$\mathrm{D_{FD}}$ [$\mathrm{cm^2/s}$]	$\mathrm{D_{erf}}$ [$\mathrm{cm^2/s}$]	$\mathrm{D_{LLS}}$ [$\mathrm{cm^2/s}$]
1	500	5.54×10^{-6}	5.57×10^{-6}	3.97×10^{-7}
2	500	5.18×10^{-6}	4.79×10^{-6}	-2.84×10^{-5}
3	500	5.67×10^{-6}	5.11×10^{-6}	-6.58×10^{-6}
4	250	4.98×10^{-6}	7.22×10^{-6}	-2.57×10^{-6}
fitting method		non-linear least squares		linear least squares
fluid velocity		Stokes flow	uniform	Stokes flow

For the 500μm wide channel data, $\mathrm{D_{erf}}$ matches $\mathrm{D_{FD}}$ and is also close to $\mathrm{D_{AR}}$. However, for the 250μm wide channel data $\mathrm{D_{erf}}$ no longer matches $\mathrm{D_{AR}}$ nor $\mathrm{D_{FD}}$. The degradation of the accuracy of the $\mathrm{D_{erf}}$ estimate for narrower channels can be explained by the decreased validity of the uniform fluid velocity assumption that underlies the method presented in section 2.6. The effect of reducing the validity of the uniform fluid velocity assumption for narrow channels is made very clear in Figure 2. While the finite-differences based model from section 2.5 retains its ability to match the concentration profile along the output channel, the best fit produced by the uniform fluid velocity model gets clearly worse from Figure 2b) to Figure 2c).

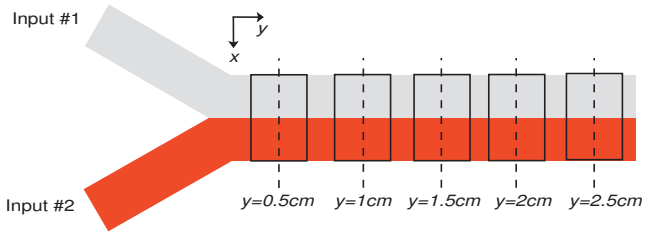

a) Schematic of top view of the channel.

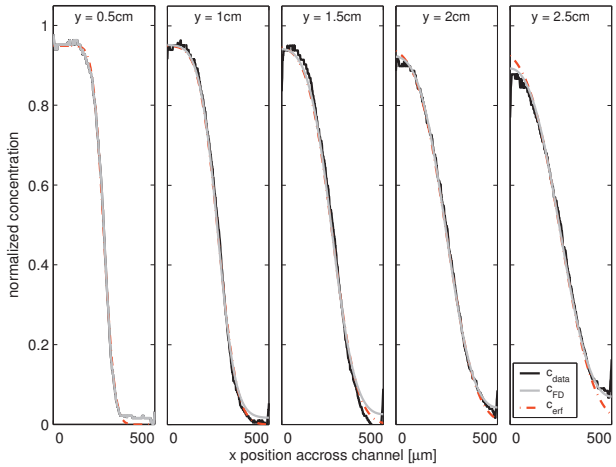

b) 500μm wide channel

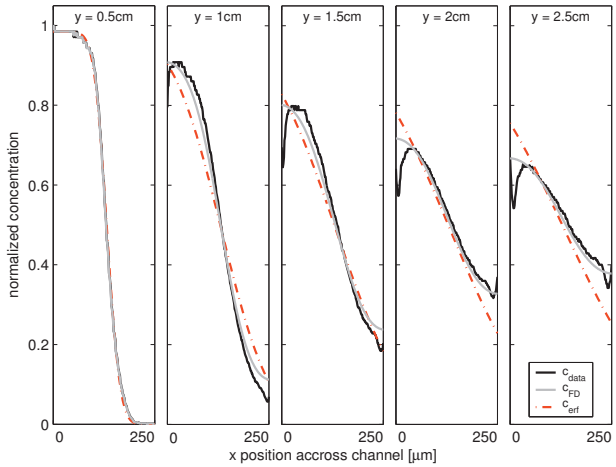

c) 250μm wide channel

Figure 2: Measured and simulated concentration profiles along the mixer output channel. The measured data is labeled c_{data}. The profiles c_{FD} were generated using non-uniform fluid velocity values and a finite differences solver (see section 2.5). The profiles c_{erf} were calculated by assuming a uniform fluid velocity profile (see section 2.6).

4 CONCLUSIONS

We have showed that, for estimating the diffusion coefficient D, solving the non-linear least squares problem $D_{\mathrm{FD}} = \mathrm{argmin}(\|\mathbf{E}(D) = \mathbf{c}_{\mathrm{FD}}(D) - \mathbf{c}_{\mathrm{m}}\|_2)$ where $c_{\mathrm{FD}}(D)$ is an easily differentiated non-linear function relating spatial concentration to the diffusion constant D and $\mathbf{c}_{\mathrm{m}}$ is the set of measured concentration values, is far more robust than solving the much cheaper linear least-squares problem $\mathrm{D}_{\mathrm{LLS}} = \mathrm{argmin}(\|\tilde{\mathbf{E}}(D) = D\nabla^2\mathbf{c}_{\mathrm{m}} - \mathbf{u}\cdot\nabla\mathbf{c}_{\mathrm{m}}\|_2)$.

We conclude that the process of estimating $\mathrm{D}_{\mathrm{LLS}}$ is flawed because applying ∇^2 and ∇ to the measured data severely damps the low frequency spectrum of $\mathbf{c}_{\mathrm{m}}$ and greatly amplifies the high frequency, noisy spectrum of $\mathbf{c}_{\mathrm{m}}$. Since diffusion is a smoothing process, the information required to estimate D, is bound to be associated with the lower components of the spectrum. Because it amplifies the importance of noise and reduces the importance of the relevant data, minimizing the cost function $\|\tilde{\mathbf{E}}(D_{\mathrm{LLS}})\|_2^2$ produces estimates $\mathrm{D}_{\mathrm{LLS}}$ that are inconsistent and usually meaningless.

Finally, we conclude that, especially for narrow channels, the uniform fluid velocity model described in section 2.6 is not accurate enough and that the more detailed model proposed in section 2.5 should be used.

In the future we intend to apply our estimation methods to more complicated geometries. We also plan to work on improving our experimental process to allow for a more rigorous validation of our simulation results. Important changes to the experimental procedure would be using monochromatic light sources and lens filters such that Beer-Lambert's law can be applied directly to the image data. Another important change would be replacing the gravity driven flow devices by more reliable devices driven by syringe pumps.

This work was supported by the National Science Foundation, the Singapore MIT Alliance and the Portuguese Foundation for Science and Technology.

REFERENCES

[1] Debashis Dutta and David T. Leighton Jr. Dispersion reduction in pressure-driven flow through micro-etched channels. *Anal. Chem.*, 73:504–513, 2001.

[2] Xiaoxia Bai, Jacques Josserand, Henrik Jensen, Joel S. Rossier, and Hubert H. Girault. Finite element simulation of pinched pressure-driven flow injection in microchannels. *Anal. Chem.*, 74:6205–6215, 2002.

[3] Abraham D. Strook, Stephan K. W. Dertinger, Armand Ajdari, Igor Mezic, Howard A. Stone, and George M. Whitesides. Chaotic mixer for microchannels. *Science*, 295:647–650, 2002.

[4] MIT. *Quantitative Physiology: Cells and Tissues - MicroFluidics Project Laboratory*, Fall 2004.

[5] Xin Wang. *FastStokes: A Fast 3-D Fluid Simulation Program for Micro-Electro-Mechanical Systems*. PhD thesis, MIT, June 2002.

[6] Thomas Fischer Weiss. *Cellular Biophysics: Transport*. MIT Press, Cambridge, MA, 1995.